SciMedCentral
Bringing Excellence in Open Access

Journal of Embryology & Developmental Biology

Original Research Article

Precise Level of Cnbp is Required for Proper Rostral Head Development in Zebrafish

María Antonela Sdrigotti†, Andrea María Julia Weiner†, Nora Beatriz Calcaterra*

Instituto de Biología Molecular y Celular de Rosario (IBR), Consejo Nacional de Investigaciones Científicas y Técnicas (CONICET) - Facultad de Ciencias Bioquímicas y Farmacéuticas, Universidad Nacional de Rosario (UNR), Ocampo y Esmeralda, (S2000EZP) Rosario, Argentina

† These authors have contributed equally

***Corresponding author**
Nora B. Calcaterra, IBR (CONICET-UNR), Ocampo y Esmeralda, (S2000EZP) Rosario, Santa Fe, Argentina
Tel: +54-341-423 7070 ext. 655; Fax: +54-341-4390465
Email: calcaterra@ibr-conicet.gov.ar

Submitted: 03 May 2017
Accepted: 18 July 2017
Published: 15 August 2017

Keywords
- Embryogenesis
- Zebrafish
- Neural crest
- Tol2 transgenesis
- Craniofacial cartilages

Abstract

Cellular nucleic-acid binding protein (Cnbp) is a highly conserved protein involved in both transcriptional and translational regulation of several genes. Knockout and knockdown studies suggest that Cnbp is required for proper craniofacial cartilages development. Here we provide a new insight into the influence of Cnbp dose on rostral head formation by overexpressing the wild-type Cnbp or a dominant negative mutant in both transient and stable transgenic approaches. The expression of neural crest marker genes and the development of craniofacial cartilages were adversely affected in either dominant negative or wild-type Cnbp transiently overexpressing specimens. The development of other embryonic structures was not affected neither by dominant negative or wild-type Cnbp overexpression, thus ruling out unspecific defects caused by the ectopic expression of Cnbp or its mutant. Results indicate that delimited level of Cnbp is required for proper rostral head development in zebrafish. Tol2-mediated transgenesis yielded up to 50% of stable wild-type Cnbp and 5% of dominant negative mutant overexpressing lines. Unlike observed in transient overexpression experiments, F2 offspring developed with no differences between controls and either of the two stable transgenics. Noteworthy, Cnbp levels in transiently overexpressing embryos were significantly higher than those ones measured in stable transgenics. Results suggest that stable transgenics derive from progenitors expressing constrained Cnbp levels.

Abbreviations: ssDNA: Single-Stranded DNA; **UTR**: Untranslated Region; **IRES**: Internal Ribosome Entry Site; **PEST**: Proteolytic Signal-containing Nuclear Protein; **NLS**: Nuclear Localization Signal; **EF1a**: Elongation Factor-1 alpha; **MHB**: Midbrain-Hindbrain Border; **CNC**: Cranial Neural Crest; **WISH**: Whole-mount In Situ Hybridization; **MBT**: Mid-Blastulae Transition; **ODC**: Ornithine Decarboxylase; **TOP-mRNAs**: Terminal Oligopyrimidine-mRNA

INTRODUCTION

Cnbp (cellular nucleic-acid binding protein, formerly ZNF9) is an 18 kDa single-stranded nucleic acid binding protein that binds G-rich single-stranded DNA (ssDNA) as well as RNA molecules. Binding to DNA, Cnbp is able to both suppress and enhance transcriptional expression [1-3]; binding to RNA, Cnbp modulates the translation of particular proteins by binding to 5'UTRs [4,5], IRES [6-8] and long non-coding RNAs [9]. Likely, Cnbp performs this broad spectrum of actions by acting as nucleic acid chaperone [10,11].

Cnbp homologs have been found in animals, protists and yeasts, but not in plants or bacteria [1]. Cnbp shows a high degree of identity among vertebrates but lower values among other eukaryotic sequences [12]. The totality of Cnbp amino acid sequences reported so far possess a conserved modular structure made of seven tandem CCHC zinc knuckle repeats joined by short peptide linkers. The linker between the first and second CCHC domain contains an RGG box [1]. The deletion of the first CCHC-Zn knuckle and the RGG box leads to a protein ($Cnbp_{\Delta 1\text{-}RGG}$) that conserves a slight capability to bind *in vitro* to ss-DNA, but fails to bind to RNA and act as nucleic acid chaperone [10]. Overexpression of $Cnbp_{\Delta 1\text{-}RGG}$ in *Xenopus laevis* embryos adversely affects the expression of neural crest maker genes, revealing a dominant negative effect *in vivo* [10]. Cnbp contains a putative PEST (Pro, Glu, Ser or Thr-enriched) proteolysis region adjacent to the RGG box; thus, it was suggested that controlled proteolysis might play a regulatory role [1]. Consistent with its dual role as transcriptional and translational regulator, a dual nuclear-cytoplasm localization for Cnbp has been reported [12-15]. A putative nuclear localization signal (NLS) within the third and fourth CCHC zinc knuckles was found *in silico* [13]. Recently, it has been shown that the phosphorylation of a conserved amino acid residue is involved in nuclear localization [2]. However, due to the small size of Cnbp, the existence of regulated nucleus-cytoplasmic shuttling is still under discussion.

Cnbp has been widely related to the human disease myotonic dystrophy type 2 (DM2), which is caused by an unstable CCTG tetranucleotide within the first intron of the human *CNBP* gene. Experimental evidence supports an RNA gain-of-function mechanism in which expanded CCUG-containing transcripts accumulate in the cell nuclei as foci and are responsible for the pathologic features [16]. However, our knowledge about the biological functions of Cnbp comes mainly from studies

on vertebrate gametogenesis and embryogenesis. Regarding gametogenesis, it was reported in *Carassius auratus gibelio* that Cnbp is associated with follicular cells and oocytes, being its expression higher in regenerating ovarian cysts [17]. Cnbp expression in spermatogonia is stronger than in primary and secondary spermatocytes, barely detected in spermatids, and absent in sperm [15]. During embryogenesis, Cnbp is required for proper forebrain induction and specification [14,18-21]. Consistent with these observations, *cnbp* has been recently reported as involved in Treacher Collins Syndrome (TCS, OMIM #154500) [22,23], a congenital disease characterized by craniofacial defects, including hypoplasia of facial bones, cleft palate and palpebral fissures [24].

Here we provide new insight into the influence of Cnbp dosage on zebrafish embryonic development by overexpressing the wild-type ($Cnbp_{wt}$) Cnbp or a dominant negative mutant ($Cnbp_{\Delta 1\text{-}RGG}$) in transient or stable transgenic approaches. Our results provide evidence that appropriate level of Cnbp is critical for proper rostral development. Lower than the minimum or higher than the maximum level of Cnbp expression adversely affects embryonic development.

MATERIALS AND METHODS

Ethics statement for animal care

All embryos were handled according to relevant national and international guidelines. Protocols were approved by the Comité Institucional para el Cuidado y Uso de Animales de Laboratorio (CICUAL), Facultad de Cs. Bioquímicas y Farmacéuticas-UNR, which has been accepted by the Ministerio de Salud de la Nación Argentina.

Fish and embryo rearing

Adult zebrafish were maintained at 28°C on a 14:10 h light:dark cycle as previously described [25]. Usually, two males and four females were setup in the same spawning tank. All embryos were staged according to development in hours or days post-fertilization (hpf or dpf, respectively) at 28°C [26]. Stocks of wild-type zebrafish inbred in our aquarium for more than 20-generations were used.

Plasmid constructions

$Cnbp_{wt}$ and $Cnbp_{\Delta 1\text{-}RGG}$ zebrafish cDNAs were obtained by RT-PCR with the following primers: 5'$CNBP_{wt}$ ACGTGTCGACATGGACATGAGTACCAGTGAG, 5'$Cnbp_{\Delta 1\text{-}RGG}$ GCGTCGACATGCTGTTCTGTTACCGGTGT, and 3'Cnbp CGGGATCCCGCGCGGACGCTTCGAT. cDNAs were cloned in *SalI* and *BamHI* sites in the pT2AL200R150G vector [27]. Constructs were sequenced by the DNA Sequencing Facility of University of Maine, USA. The mRNA coding for Tol2 transposase was *in vitro* transcribed from pCS2-TP plasmid [28] using mMESSAGE mMACHINE® SP6 Transcription Kit (Ambion) following the manufacturer instructions. Tol2 transposase-mRNA concentration was measured at 260 nm.

Generation and scoring of transiently expressing embryos

Five nl of purified, undigested pT2AL200R150G vector containing the EF1a:$cnbp_{wt}$-EGFP or EF1a:$cnbp_{\Delta 1\text{-}RGG}$-EGFP fusion proteins at a concentration of 100 ng/µl in water were injected into 1-cell staged wild-type embryos using glass capillaries made with a Narishige Instruments needle puller. EGFP expression was initially observed in live embryos using a fluorescent dissecting Microscope Olympus MVX10. Non-fluorescent embryos were identified and discarded at 24 hpf. Cohorts of at least 35 EGFP-positive embryos were examined in detail to compile an overall expression profile for each construct, specially registering to fluorescence subcellular location under confocal microscopy using a Confocal Zeiss LSM880 microscope. Injected embryos were observed at 10, 24, and 48 hpf for EGFP expression and then raised to adulthood.

Generation and scoring of stable transgenic lines

EF1a:$cnbp_{wt}$-EGFP and EF1a:$cnbp_{\Delta 1\text{-}RGG}$-EGFP germline stable transgenic zebrafish lines were generated by microinjecting 5 nl of a mix containing 2.5 nl of 25 ng/µl plasmid DNA plus 2.5 nl of 25 ng/µl of *in vitro* transcribed mRNA coding for transposase [29] into 1-cell staged wild-type embryos. Injected embryos with EGFP expression were identified at 24 hpf and the individuals with the highest contribution of EGFP fluorescence (approximately 25% of EGFP positive embryos) were raised to adulthood. Subsequent crossing with wild-type fish enabled identification of founder germline transgenics for individual lines following observation of non-mosaic EGFP expression in F1 and F2 embryos. EGFP expression was monitored and documented using a NIKON TE2000-E with a head eclipse C1-si confocal microscope.

Alcian blue staining

Three dpf larvae were fixed in 4% (w/v) paraformaldehyde (PFA) in phosphate-buffered saline 1X (PBS) with 0.1% (v/v) Tween-20 (PBT 1X), and washed in PBT 1X four times. The protocol detailed elsewhere was followed [30]. Pictures of cartilage staining larvae were taken with a BH2 Olympus Microscope and Nikon DS-Fi1 digital camera. Cranial cartilage measurements were determined using the ImageJ software (National Institutes of Health, Bethesda, MD, USA) [31].

mRNA *in situ* hybridization

Embryos were staged and fixed overnight in 4% (w/v) PFA in PBS 1X at 4°C. After washing, embryos were stored in methanol at -20°C until their use. The procedure for whole-mount *in situ* hybridizations was carried out as previously described [21]. Digoxigenin-uracil triphosphate-labeled riboprobes were prepared according to the manufacturer's instructions (Roche Diagnostics, Mannheim, Germany). Microscopic documentation was performed with a BH2 Olympus Microscope and a Nikon DS-Fi1 digital camera.

RNA extraction and RT-qPCR analysis

Total RNA from embryos at different developmental stages

was obtained using TRIZOL® Reagent (Invitrogen) following the manufacturer's instructions. Purified RNA was incubated with RQ1 DNAse (Promega) and used to perform RT-qPCR. Total RNA was retro-transcribed with SuperScript II enzyme (Invitrogen) using oligo(dT) primer. Reactions were performed with four different RNA purifications and three independent experiments using an Eppendorf Realplex2 and standard temperature protocol. Primers for *Cnbp*$_{wt}$ and *Cnbp*$_{\Delta 1\text{-}RGG}$ were: Forward, GCTTTGGGCACATCCAGAAAT; Reverse: CCGCAGTTGTAGCAGTTCAC. Predictable PCR products span at least one intron, to ensure amplification solely from the cDNA and not from genomic DNA. *rpl13α* was used as endogenous control for normalization analysis. Primer sequences for *rpl13α* were: Forward, TCTGGAGGACTGTAAGAGGTATGC; Reverse: AGACGCACAATCTTGAGAGCAG. Data were analyzed using qBase software version 2.2.

Statistics

t-student tests were employed as indicated. For qPCR, statistical analysis was performed with GraphPad Prism software, version 5.03.

RESULTS

Transient overexpression of both wild-type and dominant negative Cnbp forms adversely affects rostral head development

In order to get insight into the role of Cnbp in embryonic development, we assessed the effects of both Cnbp$_{wt}$ and Cnbp$_{\Delta 1\text{-}RGG}$ overexpression in developing zebrafish. The cDNA coding for either zebrafish Cnbp$_{wt}$ or Cnbp$_{\Delta 1\text{-}RGG}$ (Fig. 1A) were cloned under the control of the strong constitutive promoter EF1α in the pT2AL200R150G vector [27] as N-terminal fusions to EGFP, and then injected into one-cell staged zebrafish embryos. The empty plasmid was injected as control. Embryonic development was then allowed to proceed and fluorescent embryos and larvae were selected at specific developmental stages for further analyses. Percentages of mortality did not significantly differ between controls and Cnbp$_{wt}$ or Cnbp$_{\Delta 1\text{-}RGG}$ overexpressing specimens (Fig. 1B). Compared to embryos injected with the empty vector (controls, Fig. 1C), both Cnbp$_{wt}$ and Cnbp$_{\Delta 1\text{-}RGG}$ overexpression generated aberrant phenotypes (Fig. 1D-G, only representative pictures of Cnbp$_{wt}$ larvae are shown). Constructs were similar to those formerly reported for Cnbp morphants [19,20]. Phenotypes were classified as dead (coagulated, not shown), weak (Fig. 1D-E) or severe (Fig. 1F-G). Weak phenotypes were characterized by developmental delay, aberrant development of the midbrain hindbrain border (MHB), changes in pigmentation, and mild craniofacial malformations (e.g., slight alterations in the shape or size of the head, in the shape or development of the mouth; alterations in the size of the eyes). In these specimens, neither somitogenesis nor otic vesicle development were affected by Cnbp$_{wt}$ and Cnbp$_{\Delta 1\text{-}RGG}$ overexpression (Fig. 1D-C), thus ruling out non-specific defects caused by the ectopic expression of Cnbp or its mutant. Specimens classified as presenting severe phenotypes displayed malformations in neural crest derivatives, such as defective heart, smaller or even fused eyes, or strong craniofacial defects (Fig. 1F-G). Larvae displaying stronger phenotypes did not develop further than 6 dpf (not shown).

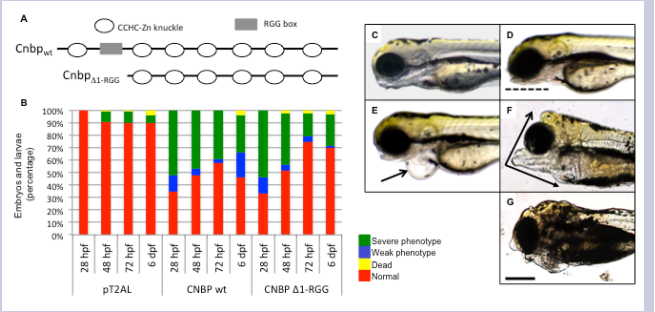

Figure 1: Cnbp$_{wt}$ and Cnbp$_{\Delta 1\text{-}RGG}$ transient overexpression causes similar developmental phenotypes. (A) Scheme of Cnbp$_{wt}$ and Cnbp$_{\Delta 1\text{-}RGG}$ proteins showing their main domains; white ovals represent the CCHC-Zn knuckle domains and the grey rectangle the RGG box domain. (B) Stacked bar graph showing phenotypic results from Cnbp$_{wt}$ and Cnbp$_{\Delta 1\text{-}RGG}$ transient overexpression in percentage (%). Results of normal (red), dead (yellow), weak (blue), and severe (green) phenotypes are shown for the four developmental stages analysed and for each of the three treatments. (C-G) Phenotypes of 72 hpf control (C) and overexpressing Cnbp$_{wt}$ larvae; (D-E) weak phenotype; (F-G) severe phenotype. Black dashed line in D highlights mandibular malformations; black arrow in E shows oedema, and black arrows in F show severe head malformations. All pictures correspond to lateral views with cephalic region to the left. Scale bar: 250 µm.

We further characterized the craniofacial cartilage pattern of Cnbp$_{wt}$ and Cnbp$_{\Delta 1\text{-}RGG}$ overexpression in 3 dpf larvae by Alcian blue staining (representative results and images of Cnbp$_{\Delta 1\text{-}RGG}$ overexpression are shown in Fig. 2). Overexpression of both Cnbp$_{wt}$ and Cnbp$_{\Delta 1\text{-}RGG}$ caused shortening of Meckel (M), ceratohial (CH) and hyosymplectic-palatoquadrate (PQ) lengths. The Meckel area (defined as the area of triangle shaped by the Meckel cartilages), the distance between ceratohyal cartilages joint and lateral fins, and the cranial distance (measured as the distance from the anterior-most M and lateral fins) also showed significant reductions (Fig. 2A-F; N=32). Moreover, angles formed by Meckel and ceratohyal cartilages were significantly more obtuse than in controls (Fig. 2B, compare D with F). These types of measurements have been used by us [23] and others [24] to describe craniofacial phenotypes affecting cartilages. In the case of more severe phenotypes, profound disorganization of cartilages precluded a detailed study (Fig. 2G). As most of the craniofacial cartilages derive from cranial neural crest (CNC) [32,33], the CNC marker genes *foxd3* and *tfap2a* were analyzed by whole-mount *in situ* hybridization (WISH) in overexpressing embryos. Data revealed changes in the expression pattern of both genes (Fig. 3A-F'), which resembled the ones detected in *cnbp* knockdown experiments [20]. At 12 hpf, *foxD3* expression was mainly restricted to non-migratory neural crest (NC) cells in both Cnbp$_{\Delta 1\text{-}RGG}$ and Cnbp$_{wt}$ overexpressing embryos (Fig. 3A-C", red dotted lines). At 24 hpf, *tfap2a* expression was barely detected in notochord, epidermis and pronefric ducts in Cnbp$_{wt}$ or Cnbp$_{\Delta 1\text{-}RGG}$ overexpressing embryos (Fig. 3D-F). Changes in spatial *tfap2a* expression was also detected at telencephalon migratory CNC of posterior brain (Fig. 3D'-F'). No significant changes in the expression pattern of *sox10* were observed in 24 hpf-staged embryos (Fig. 3G-I"), in agreement with previous results showing that *cnbp* knockdown does not affect the development of non-ectomesenchymal NC derivatives [20]. The expression pattern

of *myoD* did not show detectable variations (Fig. 3J-L'), further substantiating the role of Cnbp in rostral head development and the notion that the defects are not caused by the ectopic expression of Cnbp or its mutant form.

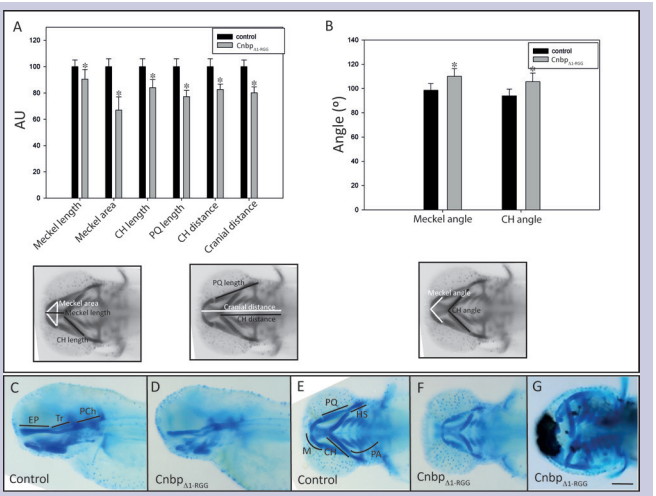

Figure 2: Cnbp$_{\Delta 1\text{-}RGG}$ overexpression adversely affects craniofacial cartilages development. (A) Bar graph showing the quantification, in arbitrary units (AU), of craniofacial parameters measured in control and Cnbp$_{\Delta 1\text{-}RGG}$ overexpressing 3-dpf larvae. Meckel length, distance between Meckel cartilage and ceratohyal cartilages joint; Meckel area, area of triangle defined by the Meckel cartilage; CH length, length of ceratohyal cartilage; PQ length, length of palatoquadrate+hyosymplectic cartilages; CH distance, distance between ceratohyal cartilages joint and lateral fins; Cranial distance, distance between the most anterior Meckel and lateral fins. (B) Bar graph showing the quantification of Meckel and ceratohyal cartilage angles in control and Cnbp$_{\Delta 1\text{-}RGG}$ overexpressing 3-dpf larvae. Alcian Blue staining of head cartilages from control (C and E) and overexpressing Cnbp$_{\Delta 1\text{-}RGG}$ (D and F: weak phenotype; G: severe phenotype) 3 dpf larvae. Abbreviations: EP, ethmoid plate; Tr, trabeculae; PCh, parachordals; M, Meckel's cartilage; PQ, palatoquadrate; HS, hyosymplectic cartilage; CH, ceratohyal cartilages; PA, pharyngeal arches. In C and D: larvae in lateral views, cephalic to the left; in E-G: larvae in ventral views, cephalic to the left. One asterisk indicates p<0.001 by *t*-Student test. Scale bar: 150 µm.

Generation of stable Cnbp transgenic zebrafish lines

Because transient expression may lead to protein mosaicism, we generated either Cnbp$_{wt}$ or Cnbp$_{\Delta 1\text{-}RGG}$ overexpressing stable transgenic zebrafish lines by using the Tol2 transposon system [28]. Twenty four of the 37 fluorescent F0 specimens overexpressing Cnbp$_{wt}$ reached adulthood and were able to spawn. Eleven of these 24 specimens produced non-fluorescent offspring while 11 females and two males were heterozygous F1 Cnbp$_{wt}$-overexpressing transgenic fish (transgenesis frequency ~ 54%; Fig. 4). Heterozygous F1 fish were mated to achieve homozygous Cnbp$_{wt}$-overexpressing zebrafish. Detailed analysis of EGFP intensity revealed two different levels of EGFP expression among transgenic embryos. Therefore, two stable lines were established as *Tg(Xla.Eef1a1:cnbpa-EGFP)*^{a} and *Tg(Xla.Eef1a1:cnbpa-EGFP)*^{b} and subsequently maintained in our fish facility as representative lines. *Tg(Xla.Eef1a1:cnbpa-EGFP)*^{b} embryos had a slightly higher EGFP expression level. Differences among stable transgenic lines and controls in either sexual behavior or ability to generate offspring were not detected.

Thirty specimens injected with Cnbp$_{\Delta 1\text{-}RGG}$ reached adulthood; 19 of them generated F1 offspring. However, a single female resulted as heterozygous F1 Cnbp$_{\Delta 1\text{-}RGG}$- overexpressing transgenic zebrafish (transgenesis frequency ~ 5%;

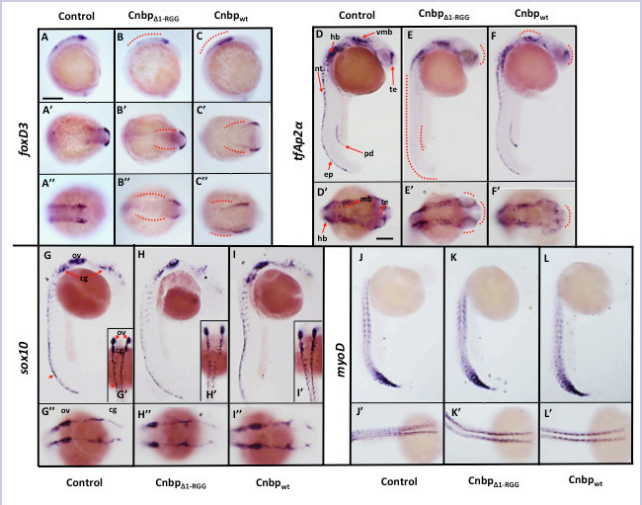

Figure 3: Transient Cnbp$_{wt}$ and Cnbp$_{\Delta 1\text{-}RGG}$ overexpression affects the expression pattern of typical NC marker genes. (A-C'') whole-mount in situ hybridization (WISH) performed on 12 hpf embryos; (D-L') WISH performed on 24 hpf embryos. Red arrows highlight the embryonic territories where the genes are expressed, while the differences in gene expression patterns are indicated with red dotted lines. Abbreviations: pd, pronefric ducts; ep, epidermis; nt, notochord; cg, cranial ganglio; mb, midbrain; vmb, ventral midbrain; hb, hindbrain; te, telencephalon; ov, otic vesicle. In A-L pictures: lateral views cephalic to the top; in A'-F', A''-C'', G''-I'', and J'-L' pictures: dorsal views cephalic to the right; in G'-I' pictures: dorsal views cephalic to the top. Scale bar: 250 µm, in A for A-C''; in D' for D-L'.

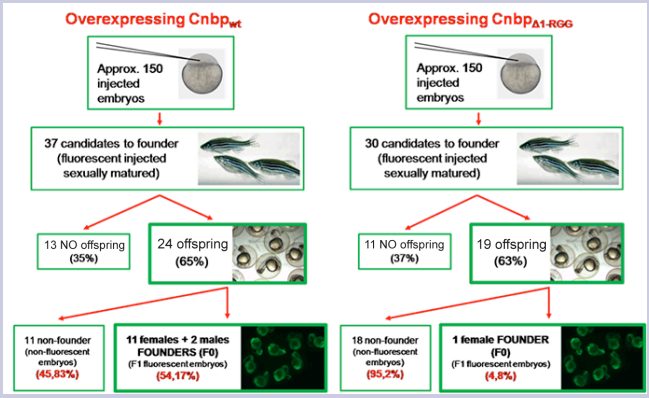

Figure 4: Scheme showing the numbers and percentages of zebrafish specimens obtained during the generation of stable transgenic lines overexpressing Cnbp$_{wt}$ and Cnbp$_{\Delta 1\text{-}RGG}$

Fig. 4). The line was maintained in our facility as *Tg(Xla.Eef1a1:cnbpa_M1-G35del-EGFP)*.

Characterization of CNBP subcellular localization in germline transgenic zebrafish embryos

Stable transgenic lines expressing EGFP fused to Cnbp allowed us to evaluate under confocal microscopy the Cnbp subcellular behavior along embryonic development. Specimens staged from 1-cell to 5-dpf displayed similar EGFP expression patterns (Fig. 5). The detection of fluorescence prior to the mid-blastula transition (MBT) indicates the maternal origin of transcripts synthetized under the control of the EF1a promoter. Previous works suggested that Cnbp shuttles between the nucleus and the cytoplasm, and localizes mostly in the nucleus after the onset of zygotic transcription [13,34]. Confocal microscopy

indeed revealed the presence of $Cnbp_{wt}$-EGFP homogeneously distributed in the cytoplasm of blastomeres prior MBT, as well as a clear nuclear localization in blastomeres in which the onset of zygotic transcription took place (Fig. 6A and B). Similar results were obtained for $Cnbp_{\Delta 1\text{-}RGG}$-EGFP transgenic embryos (Fig. 6C and D).

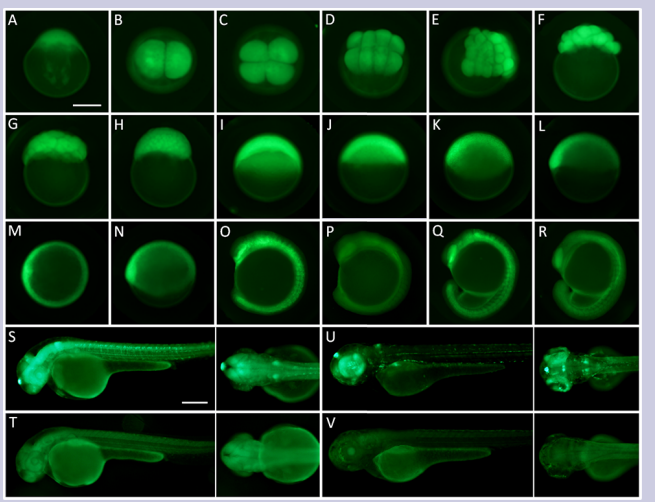

Figure 5: Fluorescence pattern displayed by $Cnbp_{\Delta 1\text{-}RGG}$ transgenic embryos at different developmental stages. (A) 1-cell, (B) 2-cells, (C) 4-cells, (D) 8-cells, (E-F): 32 cells, (G): 64-cells, (H): 256-cells, (I) sphere, (J) 30% epiboly, (K) germinal ring, (L-M) shield, (N) 70% epiboly, (O-P) 10 somite, (Q-R) 18 somite, (S-T) 42 hpf, (U-V) 60 hpf. In (A, F, G, H, I, J, K, L, and N) lateral views, animal to the top. In (O, P, Q, and R) lateral views, anterior to the top, dorsal to the right. In (B, C, D, E, and M), animal views. In (S, T, U, and V), pictures on the left are lateral views, anterior to the left and dorsal to the top; while pictures on the right are dorsal views, anterior to the left.

Cnbp dosage conditions proper rostral head development

Unlike observed in transient expression experiments, F2 offspring developed with no apparent differences between controls and either of the two stable transgenic lines. To test this, we performed WISH on stable transgenic embryos to assess the *foxD3* spatiotemporal expression pattern. At 10-somite stage, changes in spatial expression of *foxD3* were detected in both $Cnbp_{wt}$ (99%; N=41) and $Cnbp_{\Delta 1\text{-}RGG}$ (94 %; N=44) overexpressing embryos, mainly in the tailbud (Fig. 7A-C'). At 15-somite stage, *foxD3* expression pattern did not significantly change between controls (N=22) and transgenic embryos (Fig. 7D-F'; 77%; N=53). At 24 hpf, the expression of *foxD3* was barely detected in cephalic regions in both $Cnbp_{wt}$ (75%; N=44) and $Cnbp_{\Delta 1\text{-}RGG}$ (84%; N= 48) transgenic embryos (Fig. 7G-I'). Changes in craniofacial cartilages pattern between 3 dpf control and transgenics larvae were not detected (Fig. 8A-C). None of the parameters altered in transiently-overexpressing larvae were significantly altered in transgenic larvae (N= 24; not shown). To further characterize this, the expression pattern of *col2a1*, a typical marker gene of the prospective craniofacial cartilage territory, was tested in 3 dpf larvae. No differences between controls (N= 32) and transgenics (N_{wt}= 35; $N_{\Delta 1\text{-}RGG}$= 42) were detected (Fig. 8D-F).

The discrepancies between the results generated by the transient and the stable overexpression could be explained if *cnbp* expression in plasmid-injected embryos were greater than in transgenics. Thus, we measured by means of RT-qPCR the amount of $cnbp_{wt}$-mRNA and $cnbp_{\Delta 1\text{-}RGG}$-mRNA in controls, plasmid-injected, and stable transgenic embryos. Data from plasmid-injected and stable transgenic embryos were normalized to controls. The relative amount of both transcripts was significantly lower in stable transgenic embryos in most stages (Fig. 9).

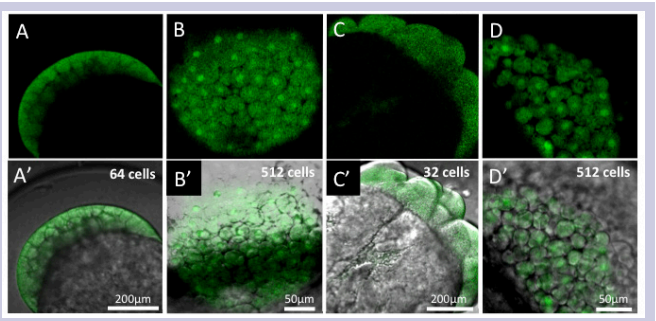

Figure 6: Cnbp subcellular location changes during embryonic development. Detection of fluorescent $CNBP_{wt}$-EGFP (A and B) and $Cnbp_{\Delta 1\text{-}RGG}$-EGFP (C and D) in the cytoplasm and nucleus of cells from transgenic embryos staged prior and after mid-blastula transition. (A'-D') Merge of images generated by transmitted light and confocal microscopy. (A and C): lateral views, animal to the top; (B and D): animal views.

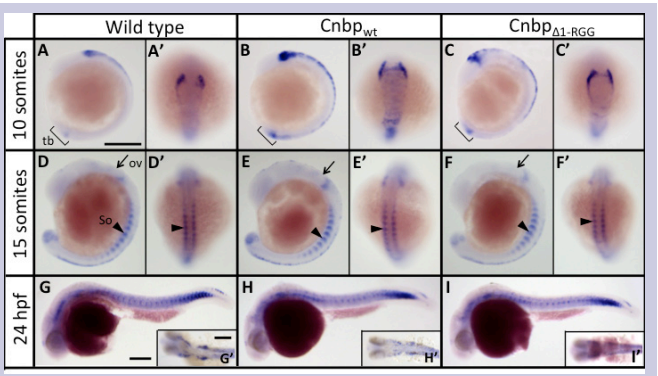

Figure 7: The expression pattern of *foxD3* is scarcely affected in stable transgenic embryos. Brackets in A, B, and C show the tailbud (tb); arrows in D, E, and F point the otic vesicle (ov); arrowheads in D-F' highlight the somites (So). In A-F pictures: lateral views, cephalic to the top and dorsal to the right. In A'-F' pictures: dorsal views cephalic to the top. In G-I pictures: lateral views, cephalic to the left. In G'-I' pictures: dorsal views cephalic to the left. Scale bar: 250 µm, in A for A-F', while in G for G-I'.

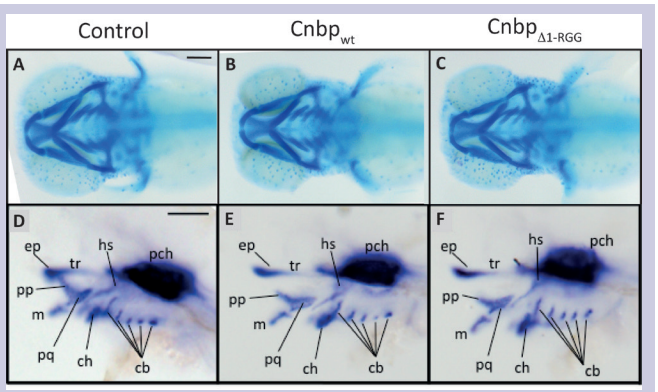

Figure 8: Craniofacial analysis in stable transgenic and control larvae. Alcian blue staining (A-C) and *Col2a1* expression pattern (D-F) in controls (A and D) and stable transgenic specimens (B-C and E-F) staged at 3 dpf. In D-F: larvae in lateral views, cephalic to the left; in D-F: larvae in ventral views, cephalic to the left. Abbreviations: bb: basibranquial, cb: ceratobranquial, ch: ceratohyal, ep: ethmoid plate, hs: hyosymplectic, m: Meckel's cartilage, pch: parachordals, pp: pterigoyd process, pq: palatoquadrate, tr: trabeculae. Scale bars: 200 µm in A for A-C; 50 µm in D for D-F. in A-C ventral view cephalic to the left.

The highest difference was detected at 75% epiboly-stage (8 hpf). At 24 hpf, the difference between the relative amount of *cnbp*$_{wt}$-mRNA in transient overexpressing and stable transgenic embryos was not significant, but the amount of *cnbp*$_{\Delta 1\text{-}RGG}$-mRNA was barely detected in stable transgenic embryos. These data further support that both low as well as high level of Cnbp adversely affects embryonic development.

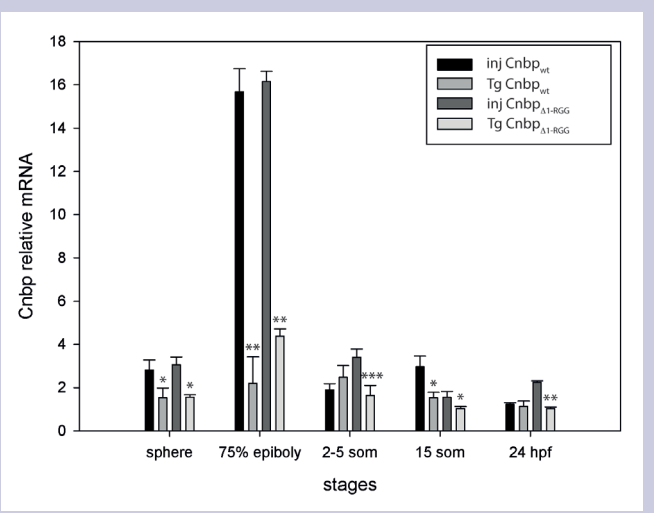

Figure 9: Transient overexpressing specimens have higher amount of *cnbp*-mRNA than the stable transgenics. Levels of both the *cnbp*$_{wt}$ and *cnbp*$_{\Delta 1\text{-}RGG}$ mRNA were measured by RT-qPCR. Significant differences were obtained between injected and transgenic embryos at some stages (labelled with asterisks). One asterisk indicates $p<0.05$, two asterisks indicate $p<0.001$, while three asterisks indicate $p<0.005$ by *t*-Student test.

DISCUSSION

In mouse, Cnbp locates in the nucleus of the early developing embryos [14]. However, both in amphibian and fish Cnbp appeared to be maternally inherited and stored as a cytoplasmic protein in oocytes and early embryos, becoming nuclear at later developmental stages [12,13,17]. The possibility of visualizing the green fluorescence of germline transgenic zebrafish enabled to confirm the cytoplasm-nuclear shift of Cnbp during embryonic development. While molecules of ~20 kDa or less freely diffuse through the nuclear pore complex, the passage of molecules above ~30 kDa (roughly the size of a EGFP molecule) requires a facilitated active transport mediated by specific proteins [35]. Both the Cnbp$_{wt}$-EGFP and Cnbp$_{\Delta 1\text{-}RGG}$-EGFP chimeras are ~45 kDa. Hence, detection of green fluorescence in the nuclei of zebrafish embryonic cells indicates that Cnbp nuclear import is a regulated transport. The similar behavior of Cnbp$_{wt}$-EGFP and Cnbp$_{\Delta 1\text{-}RGG}$-EGFP suggests that protein domains responsible for the nucleus-cytoplasm shuttling are located downstream to the RGG box in the Cnbp amino acid sequence.

Tol2-mediated transgenesis enabled the generation of stable zebrafish transgenic lines overexpressing Cnbp$_{wt}$ and the dominant negative isoform CNBP$_{\Delta 1\text{-}RGG}$. None of the stable transgenic fish displayed apparent developmental abnormalities and most of them reached adulthood being able to give normal offspring. The presence of green fluorescence in F1 embryos was the criterion for selecting candidates for transgenic lines founders, in which green fluorescence detection indicated the synthesis of fusion Cnbp$_{\Delta 1\text{-}RGG}$-EGFP and Cnbp$_{wt}$-EGFP proteins. Nevertheless, the relative amounts of mRNA coding for both chimeras in transgenic embryos were strikingly lower than those ones measured in transient overexpressing specimens staged at the same age; furthermore, from 15 somite stage onwards the expression of Cnbp$_{\Delta 1\text{-}RGG}$-EGFP was barely detected. Therefore, if Cnbp doses above a maximum or below a minimum adversely affect embryonic development, the transgenic lines will derive from progenitors expressing constrained Cnbp levels. This may also be because of the compensatory mechanisms developed in the stable line, which might be absent in the transient specimens.

Mouse wide-genome *in silico* screen has suggested the existence of polymorphisms in *cis*-elements controlling the expression of *cnbp* [36]. Cnbp expression is restricted to neuroepithelial cells [14,18,19], which exist endogenously in a highly oxidative state relative to cells in the non-neural ectoderm, mesoderm and endoderm [37]. Apart from its role in the Wnt signaling pathway [3], Cnbp prevents the redox-responsive genes up-regulation in zebrafish developing embryos subjected to oxidative stress [23]. Redox-sensitive signaling controls various cellular functions during neurogenic development, including cell proliferation and differentiation [38]. Therefore, robust control of Cnbp levels becomes crucial to guarantee not only the redox state of neuroepithelial cells but also their proliferation and differentiation in order to guarantee the normal rostral head development.

ACKNOWLEDGMENTS

We gratefully acknowledge Dr. Koichi Kawakami from Division of Molecular and Developmental Biology, National Institute of Genetics, Japan, for the generous gift of the pT2AL200R150G plasmid. We are indebted to Sebastian Graziati for expert fish care. We also thank Marcela Culasso, María Robson, Mariana de Sanctis, and Geraldine Raimundo from the English Department (FCByF) for the language correction of this manuscript. This work was supported by an ANPCyT PICT Grant (PICT-2014-1885 and PIP 2015-0170 to NBC). MAS is fellow and AMJW and NBC are Staff Members of CONICET. We are also grateful to four anonymous reviewers for their comments and peer-review.

DISCLOSURE

Neither financial interests nor conflicts of interest exist.

REFERENCES

1. NB Calcaterra, P Armas, AM Weiner, M Borgognone. CNBP: a multi-functional nucleic acid chaperone involved in cell death and proliferation control. IUBMB life. 2010; 62: 707-714.

2. E Lee, TA Lee, JH Kim, A Park, EA Ra, S Kang, HJ Choi, JL Choi, HD Huh, JE Lee, S Lee, B Park. CNBP acts as a key transcriptional regulator of sustained expression of interleukin-6. Nucleic Acids Res. 2017; 45: 3280-3296.

3. E Margarit, P Armas, N Garcia Siburu, NB Calcaterra. CNBP modulates

the transcription of Wnt signaling pathway components. Biochimica et biophysica acta. 2014; 1839: 1151-1160.

4. L Pellizzoni, F Lotti, SA Rutjes, P Pierandrei-Amaldi. Involvement of the Xenopus laevis Ro60 autoantigen in the alternative interaction of La and CNBP proteins with the 5'UTR of L4 ribosomal protein mRNA. Journal of molecular biology. 1998; 281: 593-608.

5. S Schlatter, M Fussenegger. Novel CNBP- and La-based translation control systems for mammalian cells. Biotechnol Bioeng. 2003; 81: 1-12.

6. L Antonucci, D D'Amico, L Di Magno, S Coni, L Di Marcotullio, B Cardinali, A Gulino, L Ciapponi, G Canettieri. CNBP regulates wing development in Drosophila melanogaster by promoting IRES-dependent translation of dMyc. Cell Cycle. 2014; 13: 434-439.

7. MA Sammons, AK Antons, M Bendjennat, B Udd, R Krahe, AJ Link. ZNF9 activation of IRES-mediated translation of the human ODC mRNA is decreased in myotonic dystrophy type 2. PloS one. 2010; 5: e9301.

8. VR Gerbasi, AJ Link. The myotonic dystrophy type 2 protein ZNF9 is part of an ITAF complex that promotes cap-independent translation. Mol Cell Proteomics. 2007; 6: 1049-1058.

9. Z Xue, S Hennelly, B Doyle, AA Gulati, IV Novikova, KY Sanbonmatsu, LA Boyer. A G-Rich Motif in the lncRNA Braveheart Interacts with a Zinc-Finger Transcription Factor to Specify the Cardiovascular Lineage. Mol Cell. 2016; 64: 37-50.

10. P Armas, TH Aguero, M Borgognone, MJ Aybar, NB Calcaterra. Dissecting CNBP, a zinc-finger protein required for neural crest development, in its structural and functional domains. Journal of molecular biology. 2008; 382: 1043-1056.

11. M Borgognone, P Armas, NB Calcaterra. Cellular nucleic-acid-binding protein, a transcriptional enhancer of c-Myc, promotes the formation of parallel G-quadruplexes. The Biochemical journal. 2010; 428: 491-498.

12. P Armas, MO Cabada, NB Calcaterra. Primary structure and developmental expression of Bufo arenarum cellular nucleic acid-binding protein: changes in subcellular localization during early embryogenesis. Development, growth & differentiation. 2001; 43: 13-23.

13. P Armas, S Cachero, VA Lombardo, A Weiner, ML Allende, NB Calcaterra. Zebrafish cellular nucleic acid-binding protein: gene structure and developmental behaviour. Gene. 2004; 337: 151-161.

14. W Chen, Y Liang, W Deng, K Shimizu, AM Ashique, E Li, YP Li. The zinc-finger protein CNBP is required for forebrain formation in the mouse. Development. 2003; 130: 1367-1379.

15. JX Liu, YH Zhai, JF Gui. Expression pattern of cellular nucleic acid-binding protein (CNBP) during embryogenesis and spermatogenesis of gibel carp. Mol Biol Rep. 2009; 36: 1491-1496.

16. CL Liquori, K Ricker, ML Moseley, JF Jacobsen, W Kress, SL Naylor, JW Day, LP Ranum. Myotonic dystrophy type 2 caused by a CCTG expansion in intron 1 of ZNF9. Science. 2001; 293: 864-867.

17. JX Liu, JF Gui. Expression pattern and developmental behaviour of cellular nucleic acid-binding protein (CNBP) during folliculogenesis and oogenesis in fish. Gene. 2005; 356: 181-192.

18. Y Abe, W Chen, W Huang, M Nishino, YP Li. CNBP regulates forebrain formation at organogenesis stage in chick embryos. Dev Biol. 2006; 295: 116-127.

19. AM Weiner, ML Allende, TS Becker, NB Calcaterra. CNBP mediates neural crest cell expansion by controlling cell proliferation and cell survival during rostral head development. Journal of cellular biochemistry. 2007; 102: 1553-1570.

20. AM Weiner, MA Sdrigotti, RN Kelsh, NB Calcaterra. Deciphering the cellular and molecular roles of cellular nucleic acid binding protein during cranial neural crest development. Development, growth & differentiation. 2011; 53: 934-947.

21. E Margarit, P Armas, NG Siburu, NB Calcaterra. CNBP modulates the transcription of Wnt signalling pathway components. Biochimica et biophysica acta. 2014.

22. AM Weiner, NL Scampoli, NB Calcaterra. Fishing the molecular bases of Treacher Collins syndrome. PloS one. 2012; 7: e29574.

23. MS de Peralta, VS Mouguelar, MA Sdrigotti, FA Ishiy, RD Fanganiello, MR Passos-Bueno, G Coux, NB Calcaterra. Cnbp ameliorates Treacher Collins Syndrome craniofacial anomalies through a pathway that involves redox-responsive genes. Cell Death Dis. 2016; 7: e2397.

24. DR van Gijn, AS Tucker, MT Cobourne. Craniofacial development: current concepts in the molecular basis of Treacher Collins syndrome. The British journal of oral & maxillofacial surgery. 2013; 51: 384-388.

25. M Westerfield. The Zebrafish Book. Guide for the laboratory use of Zebrafish (Danio rerio). 3rd Edition ed., University of Oregon Press., Eugene, Oregon, USA. 1995.

26. CB Kimmel, WW Ballard, SR Kimmel, B Ullmann, TF Schilling. Stages of embryonic development of the zebrafish. Dev Dyn. 1995; 203: 253-310.

27. A Urasaki, G Morvan, K Kawakami. Functional dissection of the Tol2 transposable element identified the minimal cis-sequence and a highly repetitive sequence in the subterminal region essential for transposition. Genetics. 2006; 174: 639-649.

28. K Kawakami. Tol2: a versatile gene transfer vector in vertebrates. Genome Biol. 2007; 8 Suppl 1: S7.

29. K Kawakami, H Takeda, N Kawakami, M Kobayashi, N Matsuda, M Mishina. A transposon-mediated gene trap approach identifies developmentally regulated genes in zebrafish. Dev Cell. 2004; 7: 133-144.

30. KS Solomon, T Kudoh, IB Dawid, A Fritz. Zebrafish foxi1 mediates otic placode formation and jaw development. Development. 2003; 130: 929-940.

31. CA Schneider, WS Rasband, KW Eliceiri. NIH Image to ImageJ: 25 years of image analysis. Nat Methods. 2012; 9: 671-675.

32. CB Kimmel, CT Miller, CB Moens. Specification and morphogenesis of the zebrafish larval head skeleton. Dev Biol. 2001; 233: 239-257.

33. RD Knight, TF Schilling. Cranial neural crest and development of the head skeleton. Advances in experimental medicine and biology. 2006; 589: 120-133.

34. NB Calcaterra, JF Palatnik, DM Bustos, SE Arranz, MO Cabada. Idenification of mRNA-binding proteins during development: characterization of Bufo arenarum cellular nucleic acid binding protein. Development, growth & differentiation. 1999; 41: 183-191.

35. D Mohr, S Frey, T Fischer, T Guttler, D Gorlich. Characterisation of the passive permeability barrier of nuclear pore complexes. EMBO J. 2009; 28: 2541-2553.

36. C Attanasio, AS Nord, Y Zhu, MJ Blow, Z Li, DK Liberton, H Morrison,

Plajzer-Frick, A Holt, R Hosseini, S Phouanenavong, JA Akiyama, M Shoukry, V Afzal, EM Rubin, DR FitzPatrick, B Ren, B Hallgrimsson, LA Pennacchio, A Visel. Fine tuning of craniofacial morphology by distant-acting enhancers. Science. 2013; 342: 1241006.

37. D Sakai, J Dixon, A Achilleos, M Dixon, PA Trainor. Prevention of Treacher Collins syndrome craniofacial anomalies in mouse models via maternal antioxidant supplementation. Nature communications. 2016; 7: 10328.

38. EA Ostrakhovitch, OA Semenikhin. The role of redox environment in neurogenic development. Arch Biochem Biophys. 2013; 534: 44-54.

About the Corresponding Author

Dr. Nora Beatriz Calcaterra

Summary of background:

POSITION TITLE

- Member of the Scientific National Research Council (CONICET) Career. Year: 1992-Current
- Associate Professor, Facultad Cs. Bioquímicas y Farmacéuticas, Universidad Nacional de Rosario, Rosario - Argentina. Year: 2000-Current

EDUCATION

- Universidad Nacional de Rosario - Title: Biochemist. Year: 1978 - 1983. Field of Degree: Biochemistry
- Universidad Nacional de Rosario - Title: Doctor (PhD). Year: 1984 - 1988. Field of Degree: Enzymology
- Universidad Nacional de Rosario - Postdoctoral Training; year: 1988 - 1992. Field of Degree: Plant Molecular Biology
- Centro de Biología Molecular "Severo Ochoa"; Univ. Autónoma de Madrid, Faculty of Sciences, Madrid, Spain. Visiting Professor. Year: 1997. Field of Degree: Animal Molecular Biology

Website:
http://www.ibr-conicet.gov.ar/laboratorios/calcaterra/

Current research focus:

The main goal of our laboratory is to get insight into the molecular mechanisms involved in rostral head development. We are interesting in understanding not only how the vertebrate faces develop but also how human congenital craniofacial defects arise. The approach is at two levels:

- Modelling of human craniofacial pathologies (cleft palate, aberrations in jaw and jaw formation, etc.) in the experimental zebrafish model.
- Characterization of the molecular mechanisms controlling genes expression during embryonic development: the work is foused in assessing the role of non-canonical (G-quadruplex) DNA or RNA structures and G-quadruplex-interacting proteins in the transcriptional and translational regulation of key development genes.

Permanent e-mail address: calcaterra@ibr-conicet.gov.ar

Cite this article

Sdrigotti M, Weiner A, Calcaterra N (2017) Precise Level of Cnbp is Required for Proper Rostral Head Development in Zebrafish. J Embryol Dev Biol 1(1): 1001